

Entropically stabilized growth of a two-dimensional random tiling

Andrew Stannard, Matthew O. Blunt, Peter H. Beton, and Juan P. Garrahan

School of Physics and Astronomy, University of Nottingham, University Park, Nottingham NG7 2RD, United Kingdom

(Received 19 April 2010; revised manuscript received 19 May 2010; published 12 October 2010)

The assembly of molecular networks into structures such as random tilings and glasses has recently been demonstrated for a number of two-dimensional systems. These structures are dynamically arrested on experimental time scales, so the critical regime in their formation is that of initial growth. Here, we identify a transition from energetic to entropic stabilization in the nucleation and growth of a molecular rhombus tiling. Calculations based on a lattice-gas model show that clustering of topological defects and the formation of faceted boundaries followed by a slow relaxation to equilibrium occur under conditions of energetic stabilization. We also identify an entropically stabilized regime in which the system grows directly into an equilibrium configuration without the need for further relaxation. Our results provide a methodology for identifying equilibrium and nonequilibrium randomness in the growth of molecular tilings, and we demonstrate that equilibrium spatial statistics are compatible with exponentially slow dynamical behavior.

DOI: [10.1103/PhysRevE.82.041109](https://doi.org/10.1103/PhysRevE.82.041109)

PACS number(s): 05.70.Ln, 64.60.Q–, 61.44.Br, 63.50.Lm

I. INTRODUCTION

The properties of two-dimensional supramolecular networks have been the focus of growing interest in recent years with most efforts directed toward the controlled introduction of translational order into such systems [1,2]. However, there have been several recent observations of surface-bound supramolecular arrays which assemble into dynamically arrested structures akin to glasses [3–5] which lack translational order. Such arrangements raise many interesting questions related to the growth of random systems [6,7]. In particular it is important to distinguish randomizing effects which arise from kinetic effects, such as nucleation [8,9], from equilibrium disorder due to entropic terms in the free energy. Entropically stabilized disorder may be regarded as intrinsic randomness, whereas kinetically driven disorder is often determined by sample history and preparative conditions. In one recent study [3] a random molecular rhombus tiling was shown to have equilibrium (maximum-entropy) spatial correlations, despite being frozen on an experimental time scale. In such a system the maximum-entropy configuration must form, and be frozen in, during the initial growth, since the spatiotemporal fluctuations which normally facilitate the evolution of kinetically trapped configurations to equilibrium are absent. However, it is not clear *a priori* that there is a set of local rules for molecular attachment which can lead to the direct growth of a “perfect,” i.e., maximum entropy, configuration.

In this paper we address this question and show that equilibrium and nonequilibrium effects in the growth of a rhombus tiling [10–19] may be distinguished using tile-tile correlations of arrays simulated using a lattice-gas model [20]. Direct growth to a configuration with equilibrium statistics occurs when entropic terms dominate the free energy, while nonequilibrium effects result in faceted islands and clustering of topological defects.

II. MODEL

The parameters which control growth are the tile-tile interaction energy ε , the tile adsorption energy μ , and the tem-

perature T . We consider [see Fig. 1(a)] a triangular lattice with sites, labeled i , that are either occupied by half a tile or vacant. Each rhombus tile occupies two adjacent sites and lies in one of three orientations (distinguished by different colors). For molecules deposited from solution [3] μ corresponds to the difference between the net adsorption and sol-

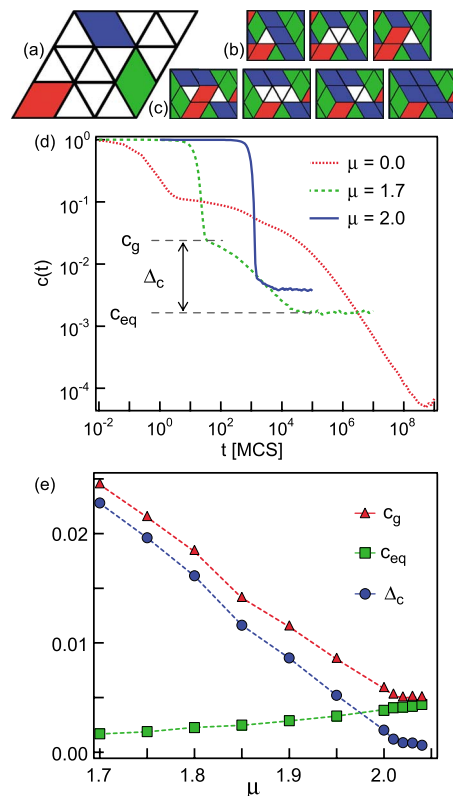


FIG. 1. (Color online) Schematic of (a) lattice and tiles; (b) defect diffusion mediated by tile detachment and reattachment; (c) annihilation of a defect pair (left to right) or generation of defect pair (right to left). (d) The fraction of empty sites as a function of time (in units of Monte Carlo sweeps) ($k_B T = 0.3$ and lattice size $N = 10^6$). (e) Dependence of c_g , c_{eq} , and Δ_c [defined in text and in (d)] on μ .

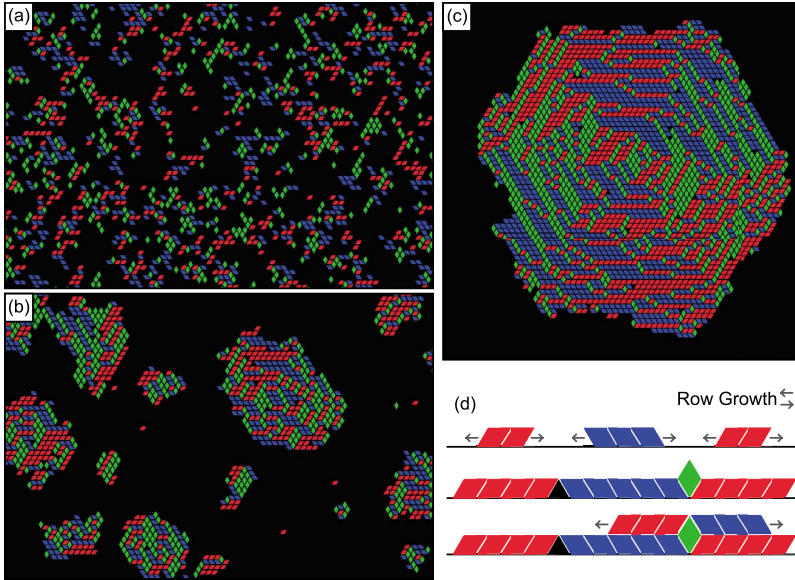


FIG. 2. (Color online) (a)–(c) Simulated growth of tilings for varying μ with $k_B T = 0.2$: (a) $\mu = 0.5$, high nucleation density, and irregular islands [$c(t) = 0.7$]; (b) $\mu = 1.5$, reduced nucleation density, and faceted islands [$c(t) = 0.7$]; (c) $\mu = 1.8$, example of an inhomogeneous tile distribution within strongly faceted island; (d) schematic of growth along a straight interface for $1 < \mu < 2$.

vation energies of the molecule ($\mu > 0$ implies a preference for solvation). The binding energy per tile for a completely tiled surface is $E_{bind} = -(2\varepsilon - \mu)$.

Using a Metropolis algorithm [21], sites are chosen randomly and, if empty, a tile is added with probability $e^{-\Delta E/k_B T}$ for $\Delta E > 0$ and with unit probability for $\Delta E \leq 0$, where ΔE is the associated change in energy. If the site is occupied, tile removal is accepted with probability $e^{-\Delta E/k_B T}/3$. The factor of $1/3$ ensures that detailed balance is satisfied. The energy required to remove a tile with p nearest neighbors is $E_{rem} = (p\varepsilon - \mu)$, which, for $\mu > 0$, may be either positive or negative depending on the local environment. One Monte Carlo sweep (MCS) corresponds to the random inspection of $3N$ sites of the (rhomboid) lattice (N is the maximum number of adsorbed tiles) and sets the unit of time. Periodic boundary conditions are used and all energies are henceforth expressed in units of ε . This is a generalization, through the introduction of the parameter μ , of a model previously used to show that rhombus tilings are glassy [20].

As the time increases, the fraction of empty lattice sites, $c(t)$, reduces from 1 (empty lattice) and eventually relaxes to an equilibrium phase at a μ -dependent constant value of $c(t)$, c_{eq} . In the initial growth phase $c(t)$ falls until an abrupt change in gradient occurs; we parametrize the value of $c(t)$ as c_g [see Fig. 1(d) where the values for c_g and c_{eq} are identified for the $\mu = 1.7$ curve]. At this point, to a good approximation, there are no more available vacancies (neighboring pairs of unfilled triangles) which could directly accommodate a tile. However, the lattice is not completely tiled and triangular void defects are also present. These are topological defects with two effective charges corresponding to triangles pointing up and pointing down [14,22,23]. Further relaxation is mediated by defect diffusion and annihilation [neighboring defects of opposite effective charges form a vacancy which may be occupied by a tile—see Fig. 1(c)] [20]. Since defect diffusion is an activated process (barrier $3 - \mu$) there is a slowing down which gives rise to the clear change in gradient discussed above. In the equilibrium regime there is a dynamic balance between the generation of triangular defect

pairs (from the removal of tiles) and their diffusion and annihilation [20]. Finally, we introduce a parameter, $\Delta c (= c_g - c_{eq})$, to quantify the difference between the defect densities in equilibrium and immediately after the initial growth phase.

III. RESULTS

The dependence of the parameters c_g , c_{eq} , and Δc on μ is shown in Fig. 1(e) over the parameter range $1.7 < \mu < 2.1$. As expected, c_{eq} increases with increasing μ since the energy barrier for tile detachment is reduced. Interestingly, in the range $\mu > 2$ the binding energy $E_{bind} > 0$, and no tiling would be expected for an ordered system. However, random tilings do grow in this regime; the variation of $c(t)$ for $\mu = 2$ is shown in Fig. 1(d), and values for c_g , c_{eq} , and Δc extracted in the regime where $E_{bind} > 0$ ($\sim 2.1 > \mu > 2$) are shown in Fig. 1(e). We show below that in this regime entropic contributions lead to a free energy F given by $(NE_{bind} - TS)$, where S is the entropy, which can be negative, favoring a tiling, even when $E_{bind} > 0$ (Joseph *et al.* [24] made similar arguments in the context of entropically stabilized quasicrystals [13,25]). Furthermore, in this entropically stabilized regime, $\Delta c \rightarrow 0$, implying—as confirmed below—that the initial growth phase leads directly to an equilibrium regime.

We now consider the differences in nucleation, morphology, and tile statistics in the energetically stabilized ($\mu < 2$) and entropically stabilized ($\mu > 2$) regimes, focusing first on low values of μ . In Fig. 2 we show islands which have been nucleated and are growing in the initial growth regime. For $0 < \mu < 1$, E_{rem} , the barrier for tile removal, is positive even for $p = 1$, indicating that any nucleated island formed by two neighboring tiles is stable (note that for $\mu \leq 0$ even isolated tiles are stable nuclei). Accordingly, the simulated growth in this regime [Fig. 2(a)] shows a large number of small irregular islands of tiles. This is an essentially homogeneous growth regime: very quickly the islands merge forming an imperfect tiling of the plane.

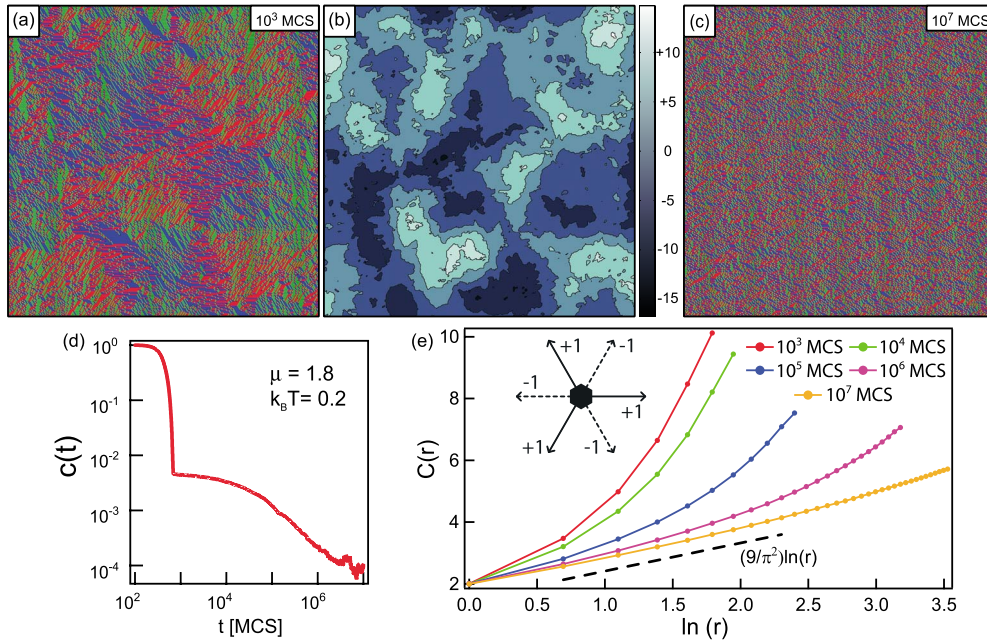


FIG. 3. (Color online) (a) An inhomogeneous tiling resulting from strongly faceted growth of multiple islands, $k_B T = 0.2$, $\mu = 1.8$, and $N = 1.6 \times 10^5$ ($\sim 4 \times 10^4$ tiles shown). (b) Clustering of topological charge shown in a charge density map. The value at a point corresponds to the number of upward-pointing minus downward-pointing defects within a range of three times the average defect separation. (c) The tiling after relaxing to an entropically maximized equilibrium state ($\sim 4 \times 10^4$ tiles shown), (d) the corresponding $c(t)$ behavior, and (e) height correlation functions during relaxation, indicating convergence to maximum randomness (top line: 10^3 MCSs; second top line: 10^4 MCSs; middle line: 10^5 MCSs; second bottom line: 10^6 MCSs; bottom line: 10^7 MCSs).

For $1 < \mu < 2$ we have heterogeneous growth; as μ increases, islands become larger and their number decreases. Furthermore, the islands that form are faceted and hexagonal [see Fig. 2(b)] with a clear deficit of tiles in one of the three possible orientations (colors) in each of the six triangular segments of the island [see Fig. 2(c)]. The faceting occurs since the smallest energetically stable nucleus requires a minimum of three tiles in a hexagonal configuration. Outward growth results in the (approximate) propagation of the hexagonal shape since growth along an edge favors the addition of a row formed by one of the two tile orientations with an edge parallel to the island boundary. For example, in Fig. 2(d), rows of blue (top-left to bottom-right long axis) and/or red (bottom-left to top-right long axis) tiles grow, and where they meet an upward- or downward-pointing triangular defect is formed. The downward defect is trapped, but the upward defect may be occupied by a green (vertical long axis) tile, leading to an excess of defects of one effective charge (downward pointing in this case) in each segment. Inspection of the hexagonal island in Fig. 2(c) shows rows of tiles of two colors with either defects or a tile of the third color where they meet, consistent with this simple explanation. Thus, the faceting is due to minimization of the boundary energy, but also results in clustering of defects with the same effective charge. A local imbalance of tiles gives rise to an increase in entropic free energy and is not expected for an equilibrium configuration. We note the interesting similarity between the growth of energetically favored hexagonal tilings observed here and the “arctic circle” problem in rhombus tilings subject to hexagonal confining boundaries [15,16].

As growth in this regime continues the islands merge while maintaining, approximately, the primordial structure introduced in the nucleation stage. An example is shown in Fig. 3(a) which shows the tiling that is formed immediately after all the growing islands merge. Defects in this tiling are not distributed uniformly as in equilibrium [19]. Figure 3(b) shows the topological charge density for the tiling of Fig. 3(a). Defect clustering is evident in the large variations in topological charge. The original nucleation sites within the tiling can be identified as singular points in this defect density [Fig. 3(b)], which confirms the spatial correlation of defect clustering and nucleation sites. Further temporal evolution governed by defect diffusion and annihilation [20] leads to equilibration of the tiling [see Fig. 3(c)] when $c(t)$ reaches its equilibrium value [see Fig. 3(d)].

The tilings are analyzed using a lifting dimension [13,26] in which an effective height $h(\vec{r})$ is assigned to each vertex (with in-plane coordinates \vec{r}) in the tiling. The height is calculated using the scheme shown in the Fig. 3(e) inset in which a displacement along a rhombus edge leads to a change in height of ± 1 . The height correlation function $C(r) = \langle [h(0) - h(r)]^2 \rangle$ can be calculated, and for a maximally random tiling, $C(r) = (\pi K_0)^{-1} \ln(r) + c$ has a logarithmic dependence on position, where c is a constant and $K_0 = \pi/9$ [13]. Figure 3(e) shows the correlation functions during the simulated growth of the tilings in Figs. 3(a) and 3(c). For the tiling in Fig. 3(a) the correlation function is not logarithmic. For increasing times the correlation functions approach a linear dependence on $\ln(r)$, with the expected gradient $9/\pi^2$, confirming that the final configuration [Fig. 3(c)] is equilibrated. This supports the hypothesis that a logarithmic de-

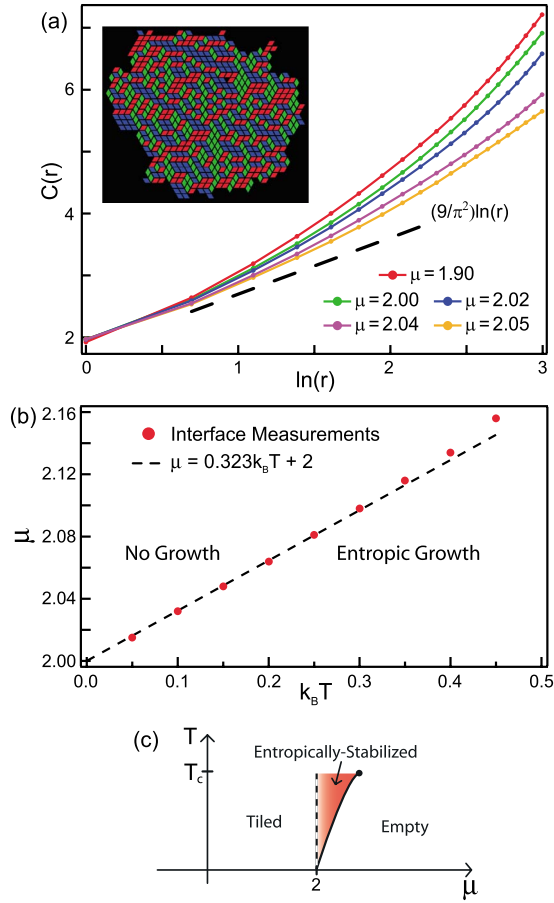


FIG. 4. (Color online) (a) Height correlation functions calculated for tilings immediately after the initial growth stage [where $c(t) = c_g$] at $k_B T = 0.3$ with varying μ (top line: $\mu = 1.90$; second top line: $\mu = 2.00$; middle line: $\mu = 2.02$; second bottom line: $\mu = 2.04$; bottom line: $\mu = 2.05$). (b) Calculations of stationary interfaces marking the tiled-untiled phase equilibrium. (c) Illustrative representation of the μ - T parameter space, indicating the region where tilings are entropically stabilized.

pendence is associated with an equilibrium configuration rather than kinetically controlled randomness, but the exponentially slow approach to equilibrium cannot account for tilings which are both dynamically arrested and maximum entropy.

For $\mu \geq 2$ nucleated islands do not show faceting or inhomogeneities [Fig. 4(a), inset], and our simulations show direct growth into a maximum-entropy configuration. In Fig. 4(a) we plot correlation functions for tilings immediately after the initial growth regime is completed [determined by the change in gradient in $c(t)$] and find an approach to a logarithmic dependence on r as μ increases. Note from Fig. 1(e) that $\Delta c \rightarrow 0$ for $\mu > 2$, and these results confirm that this simple parameter provides a reliable indicator for a regime of direct growth into an equilibrium configuration without the requirement for defect-mediated relaxation.

To confirm that tilings for $\mu > 2$ are entropically stabilized we need to establish the equilibrium phase boundary $\mu(T)$ between the tiled and empty phases. We establish this by investigating whether an interface between an equilibrated tiling and an empty lattice recedes (no growth) or propagates

(growth) [21]. The value of μ where this transition occurs is plotted against temperature in Fig. 4(b). As discussed above, for an ordered system no growth is expected for $\mu > 2$, but the free energy may be negative when $E_{bind} > 0$, if $S_{tile} > E_{bind}/T$, where S_{tile} is the entropy per tile, or $\mu < 2 + TS_{tile}$. Our simulations [Fig. 4(b)] give $S_{tile} = 0.32k_B$ in excellent agreement with the ideal value for the rhombus tiling entropy density of $0.323066k_B$ [13,27].

IV. CONCLUSIONS

These results are highly relevant to recent experiments [3]. We propose that, in both the energetically and entropically stabilized regimes, growth proceeds through the initial regime to the point identified in Fig. 1 where there is a slowing down of the evolution of the tiling. Further evolution is determined by the barrier to defect propagation, $(3 - \mu)$. If this is small compared with $k_B T$, equilibration can occur through defect propagation. However, for many molecular systems the barrier is at least an order of magnitude greater than the thermal energy, and the configuration is therefore dynamically arrested with spatial statistics which are frozen immediately after the initial tiling of the surface. A broad range of possible spatial distributions can occur, including, for $\mu \sim 2$, the recently observed maximum-entropy arrangement [3]. However, for lower values of μ a configuration with a frozen-in nonequilibrium spatial distribution of tiles [comparable to Fig. 3(a)] might be attainable in experiments.

The phase behavior observed in these simulations is summarized in Fig. 4(c) and invites analogy with magnetic Ising systems since the total energy of a partially tiled surface is given by

$$E = -\frac{\varepsilon}{2} \sum_{i=1}^{2N} n_i \left(\sum_{j=1}^3 n_j - 1 \right) + \frac{\mu}{2} \sum_{i=1}^{2N} n_i, \quad (1)$$

where $n_i = 1$ (0) for an occupied (unoccupied) site (for a related example of the application of the lattice-gas model to adsorbed molecular layers, see Ref. [28]). The index i runs over all triangular sites and j runs over the three nearest neighbors of site i . The tile-tile interaction ε is analogous to the spin-spin coupling, normally denoted by J , μ is analogous to magnetic field, and n_i to spin state. In Fig. 4(c) a boundary at $\mu = 2$ shows the threshold above which the internal energy is positive. However for $T < T_c \sim \varepsilon/k_B$ there is an entropically stabilized regime for the random rhombus tiling [shaded region in Fig. 4(c)]. This phase boundary can be determined in our simulations up to $k_B T \sim 0.5$, which we identify as an approximate critical temperature for this transition. The deposition of a molecular layer is thus equivalent to a quench from high μ (analog magnetic field). The growth dynamics after such a quench allows an investigation of this phase diagram for systems where dynamics are slow.

Our results show that equilibrium and nonequilibrium randomization may be distinguished for the rhombus tiling. Moreover, we have shown that equilibrium spatial statistics may occur even for dynamically arrested systems, although other outcomes such as faceting and defect clustering are also possible. These results have general relevance for mo-

lecular layers adsorbed at a liquid-solid interface where it has previously been assumed, correctly in many cases, that a dynamic equilibrium is established with molecules continually exchanging between solvated and adsorbed states (see [29], for example). Our results show that such an exchange is not required for the formation of maximum-entropy arrangements. There are also interesting links between entropically stabilized growth and several other problems in biophysics and condensed-matter physics, such as the crystallization of anisotropic particles [30]. Furthermore, molecular rhombus tiles provide a new system to explore, both experimentally

and theoretically, equilibrium and nonequilibrium behavior in connection with “Coulomb” and other exotic phases which can exhibit fractional excitations [26], such as frustrated magnets with effective magnetic monopoles [31], quasicrystals [7], and glasses [6,32].

ACKNOWLEDGMENTS

We thank the EPSRC for financial support through Grants No. EP/D048761/1 and No. EP/P502632/1.

-
- [1] J. A. A. W. Elemans, S. B. Lei, and S. de Feyter, *Angew. Chem., Int. Ed.* **48**, 7298 (2009).
- [2] L. Bartels, *Nat. Chem.* **2**, 87 (2010).
- [3] M. O. Blunt *et al.*, *Science* **322**, 1077 (2008).
- [4] R. Otero *et al.*, *Science* **319**, 312 (2008).
- [5] M. Marschall *et al.*, *Nat. Chem.* **2**, 131 (2010).
- [6] S. F. Swallen *et al.*, *Science* **315**, 353 (2007).
- [7] L. Bindi, P. J. Steinhardt, N. Yao, and P. J. Lu, *Science* **324**, 1306 (2009).
- [8] R. Q. Hwang and M. C. Bartelt, *Chem. Rev.* **97**, 1063 (1997).
- [9] H. Brune, *Surf. Sci. Rep.* **31**, 125 (1998).
- [10] M. E. Fisher, *Phys. Rev.* **124**, 1664 (1961).
- [11] P. W. Kasteleyn, *J. Math. Phys.* **4**, 287 (1963).
- [12] H. W. J. Blöte and H. J. Hilhorst, *J. Phys. A* **15**, L631 (1982).
- [13] C. L. Henley, in *Quasicrystals: The State of the Art*, edited by P. J. Steinhardt and D. P. Divincenzo (World Scientific, Singapore, 1999).
- [14] M. E. Fisher and J. Stephenson, *Phys. Rev.* **132**, 1411 (1963).
- [15] N. Destainville, *J. Phys. A* **31**, 6123 (1998).
- [16] H. Cohn, R. Kenyon, and J. Propp, *J. Am. Math. Soc.* **14**, 297 (2001).
- [17] N. Destainville *et al.*, *J. Stat. Phys.* **120**, 799 (2005); M. Widom *et al.*, *ibid.* **120**, 837 (2005).
- [18] A. V. Shutov and A. V. Maleev, *Acta Crystallogr., Sect. A: Found. Crystallogr.* **64**, 376 (2008).
- [19] J. L. Jacobsen and F. Alet, *Phys. Rev. Lett.* **102**, 145702 (2009).
- [20] J. P. Garrahan, A. Stannard, M. O. Blunt, and P. H. Beton, *Proc. Natl. Acad. Sci. U.S.A.* **106**, 15209 (2009).
- [21] M. E. Newman and G. T. Barkema, *Monte Carlo Methods in Statistical Physics* (Oxford University Press, Oxford, 1999).
- [22] J. Linde, C. Moore, and M. G. Nordahl, *Discrete Math. Theor. Comput. Sci. Proc. AA (DM-CCG)* **AA**, 23 (2001).
- [23] W. Krauth and R. Moessner, *Phys. Rev. B* **67**, 064503 (2003).
- [24] D. Joseph and V. Elser, *Phys. Rev. Lett.* **79**, 1066 (1997); see also P. Kalugin, *Eur. Phys. J. B* **18**, 77 (2000).
- [25] M. Widom, D. P. Deng, and C. L. Henley, *Phys. Rev. Lett.* **63**, 310 (1989).
- [26] C. L. Henley, *Annu. Rev. Condens. Matter Phys.* **1**, 179 (2010).
- [27] G. H. Wannier, *Phys. Rev.* **79**, 357 (1950); *Phys. Rev. B* **7**, 5017(E) (1973).
- [28] C. Tao *et al.*, *Proc. Natl. Acad. Sci. U.S.A.* **105**, 16418 (2008).
- [29] S. De Feyter and F. C. De Schryver, *Chem. Soc. Rev.* **32**, 139 (2003).
- [30] S. Whitelam, *J. Chem. Phys.* **132**, 194901 (2010).
- [31] C. Castelnovo, R. Moessner, and S. L. Sondhi, *Nature (London)* **451**, 42 (2008).
- [32] D. Chandler and J. P. Garrahan, *Annu. Rev. Phys. Chem.* **61**, 191 (2010).